EVALUATION OF THE ELECTRON DENSITY OF STATES IN A SI-SIO$_2$ INTERFACE USING THE ZERO-TEMPERATURE GREEN'S FUNCTION FORMALISM[1]

Dragica Vasileska-Kafedziska, Paolo Bordone[2] and David K. Ferry
Center for Solid State Electronics Research, Arizona State University
Tempe, Az, 85287-6206, USA

Abstract

We develop the zero-temperature Green's function formalism to study transport in Si-SiO$_2$ inversion layer subject to both impurity and surface-roughness scattering. Surface-roughness is treated as a random potential scattering with a Gaussian correlation function. For the sake of simplicity, we assume that the electrons are scattered by randomly located but identical δ-function impurity potentials. The position of the subband minima and the electron concentration have been obtained by the self-consistent solution of the Poisson, Schrödinger and Dyson equations for each value of the effective transverse electric field. We give the analytical expression for the broadening of the electronic states in each subband, and the expression for the conductivity that includes the correction due to the normal particle-hole ladder diagram. In addition, the numerical results for the density of states function (DOS) for various values of the effective field are given. Finally, we present the numerical results for the mobility for various fitting parameters. The results for the mobility are in agreement with the experimental results of Kawaji obtained at 4.2 K in the region where surface-roughness dominates the transport properties of the system.

I. INTRODUCTION

We study transport properties of a (100) Si-inversion layer at zero temperature. We also give the results of the numerical self-consistent calculations for the density of states function, electron density and mobility for various fitting parameters and different effective fields. The dependence of mobility on the electron concentration N_s provides information for the strength of the considered dissipative mechanisms.

Our calculations are based on two major approximations. We assume that the effective-mass approximation is valid, so that we can use the effective masses and the dielectric constants of the perfect crystal. We also assume that the envelope functions for the inversion-electrons that satisfy the one-dimensional Schrödinger-wave equation vanish in the oxide. This is a valid assumption for moderately high surface fields. At very high surface fields, the wavefunction of the first subband extends less than 1 nm in the semiconductor and in this case the approximation probably fails.

Transport properties of Si-inversion layers at low temperatures are dominated by the elastic processes such as impurity and surface-roughness scattering. Surface-roughness is important only at high effective fields, where most of the inversion-electrons are trapped in the lowest subband.

The impurities are described by a random potential $u(\mathbf{R})$ with zero mean value and a correlator

$$\langle u(\mathbf{R})u(\mathbf{R}')\rangle = n_i U_o^2 \delta(\mathbf{R}-\mathbf{R}'). \tag{1}$$

[1]Work supported in part by ONR.

[2] On leave from: Dipartimento di Fisica ed Instituto Nazionale di Fisica della Materia, Universita` di Modena, Via Campi 213/A, 41100 Modena, Italy.

where n_i is the impurity concentration. The <...> denote averaging over all impurity configurations. The strength of the impurity scattering is described through the constant U_o, equal to the matrix element for scattering from a single impurity.

Surface-roughness is introduced through a random local-potential term, proportional to the linear term of the Taylor expansion of the surface potential, of the form [1]

$$H_{sr}(\mathbf{R})=f(\mathbf{r})eE_s \quad , \tag{2}$$

where E_s is the surface field. The random function $f(\mathbf{r})$ that describes the deviation from the atomically flat surface is described by a two parameter Gaussian model, with autocorrelation function of the form

$$W_{sr}(|\mathbf{r}-\mathbf{r}'|)=\Delta^2\exp\left[-\frac{|\mathbf{r}-\mathbf{r}'|^2}{\zeta^2}\right] . \tag{3}$$

Parameters Δ and ζ characterize the root-mean-square height of the bumps on the surface and the roughness correlation length , respectively.

From the coupled Dyson's equations for the retarded Green's function, we find that, within the diagonal approximation, the broadening of the electronic states for the n-th subband is obtained as a solution of the equation

$$\Gamma_n(\varepsilon_k,\varepsilon_F)=\frac{m^*}{4\pi\hbar^2}\sum_m\int_0^\infty d\varepsilon_q a_m(\varepsilon_q,\varepsilon_F)\times$$
$$\times\left\{n_iU_o^2O_{nm}+\delta_{nm}\pi(eE_s\zeta\Delta)^2 I_o\left(\frac{m^*\zeta^2}{\hbar^2}\sqrt{\varepsilon_k\varepsilon_q}\right)\exp\left[-\frac{m^*\zeta^2}{2\hbar^2}(\varepsilon_k+\varepsilon_q)\right]\right\} . \tag{4}$$

I_o is the modified Bessel function of the zeroth order, $a_m(\varepsilon_q,\varepsilon_F)$ is the spectral density function for the m-th subband, ε_F is the Fermi energy, ε_q is the kinetic energy and O_{nm} is the overlap factor. The details of this derivation are given in [2].

Within linear response, the expression for the conductivity can be summarized as

$$\sigma=\frac{e^2}{2\pi\hbar}\sum_n(\varepsilon_F-\varepsilon_n)\int_0^\infty d\varepsilon_k\frac{a_n(\varepsilon_k,\varepsilon_F)}{\Gamma_n(\varepsilon_k,\varepsilon_F)}+\frac{e^2}{2\pi\hbar}\sum_n(\varepsilon_F-\varepsilon_n)\frac{V_n}{1-V_n}\int_0^\infty d\varepsilon_k\frac{a_n(\varepsilon_k,\varepsilon_F)}{\Gamma_n(\varepsilon_k,\varepsilon_F)} \tag{5}$$

where

$$V_n=\frac{m^*}{4\hbar^2}(eE_s\zeta\Delta)^2 e^{-\frac{m^*\zeta^2}{2\hbar^2}(\varepsilon_F-\varepsilon_n)}\int_0^\infty d\varepsilon_q\frac{a_n(\varepsilon_q,\varepsilon_F)}{\Gamma_n(\varepsilon_q,\varepsilon_F)}e^{-\frac{m^*\zeta^2}{2\hbar^2}\varepsilon_q} I_1\left[\frac{m^*\zeta^2}{\hbar^2}\sqrt{(\varepsilon_F-\varepsilon_n)\varepsilon_q}\right] . \tag{6}$$

I_1 is modified Bessel function of first order and ε_n is the subband energy. The first term on the right-hand side of (5) represents the Drude result. The second term gives the correction to the Drude conductivity due to the normal particle-hole ladder diagrams, as explained in [2]. This term yields a replacement of the relaxation time by a transport lifetime for the conduction electrons [3].

II. SIMULATION RESULTS

The self-consistent calculation of the coupled Schrödinger and Poisson equations gives the solution for the broadening of the electronic states according to (4). This is then used for the calculation of the density of states function and electron density. The process starts with an initial estimate for the potential energy profile and then solves all of the forementioned equations successively [4-6]. For the numerical solution of the Schrödinger equation, we have applied the Numerov algorithm [7], which is one order of magnitude more accurate that the fourth-order Runge-Kutta method. The matching tolerance for the wavefunctions was taken to be 10^{-5} . Finite-difference methods were used for the solution of the Poisson equation. We have used Gauss-Legendre integration for the energy integrations in (4-6) to speed the computation and decrease round-off errors.

The potential energy profile is given in Fig. 1. The Fermi energy corresponds to the zero-energy level on the figure. The electric field in the oxide is 2×10^6 V/cm. The wave-functions for the first two subbands for the lowest valleys are shown in the insert. The corresponding electric field profile, is given in Fig. 2. The spectral density function due to impurities and surface-roughness scattering is presented in Fig. 3. The fitting parameters for surface roughness are: $\Delta = 0.2nm$ and $\zeta = 1.3nm$. In the numerical simulation for the broadening of the electronic states, instead of the surface field, we have used the average field that is felt by the electrons. The field in the oxide is the same as in Figs. 1-2. In Fig. 4, we present the form of the DOS function for various oxide fields. The fitting parameters for surface-roughness are the same as above. Due to quantum-size effects, we observe a change in the slope of the DOS curves near the subband threshold. This effect is more pronounced at higher electric fields, where surface-roughness dominates the transport properties of the system. The shift in the subband energies is due to the increase of the oxide field. The mobility curve, as a function of the inversion charge density, is given in Fig. 5 . The dots represent the experimental results obtained by Kawaji at 4.2 K [4]. In the region where surface-roughness dominates the transport (high inversion charge concentration), we achieve very good agreement with the experimental data. In the other region, the fitting failed because of the assumed simplified model for impurity scattering. In order to improve the results, we need to consider the Coulomb interaction properly. From the results presented in Fig. 6, we can deduce the relationship between the average field and the inversion density. We calculate that the average electric field varies as $E_{av}=e\,(0.52N_s+N_{depl})/(\varepsilon_o\varepsilon_{sc})$.

References

[1] S. M. Goodnick, D. K. Ferry, and C. W. Wilmsen, Phys. Rev. B **32**, 8171 (1985).
[2] D. Vasileska-Kafedziska, P. Bordone, and D. K. Ferry, submitted for publication.
[3] J. Bergmann, Physics Reports **107**, No. 1 (1984), p.1 (North-Holland, Amsterdam).
[4] T. Ando, A. B. Fowler, and F. Stern, Reviews of Modern Physics **54**, 437 (1982).
[5] F. Stern, Phys. Rev. B **5**, 4891 (1972).
[6] B. Vinter, Appl. Phys. Lett. **44**, 307 (1984).
[7] S. E. Koonin and D. C. Meredith, *Computational Physics* (Addison Wesley, New York, 1990).

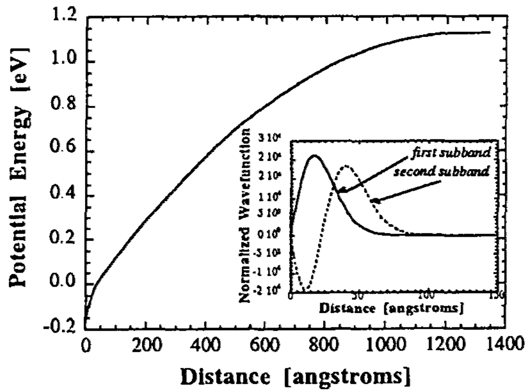

Fig.1 Potential Energy Profile

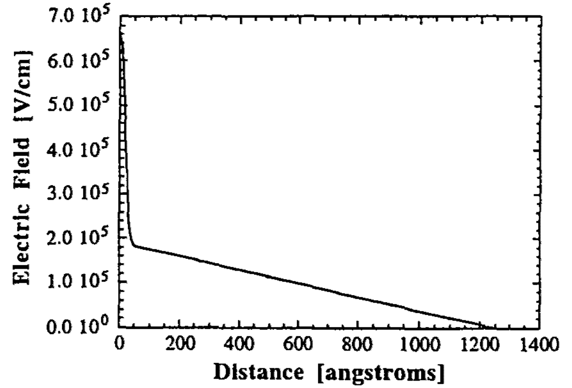

Fig.2 Electric field profile

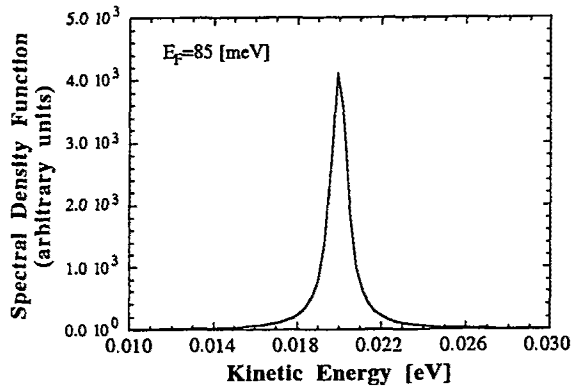

Fig.3 Spectral density function for the first subband vs kinetic energy

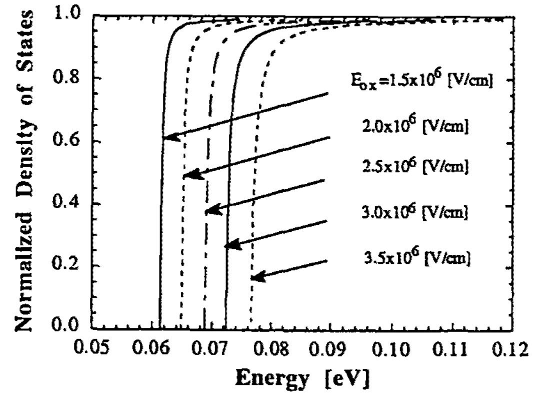

Fig.4 DOS vs Fermi energy for various oxide fields

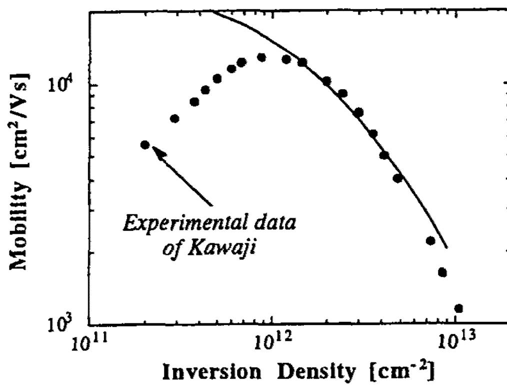

Fig.5 Calculated mobility vs inversion charge density

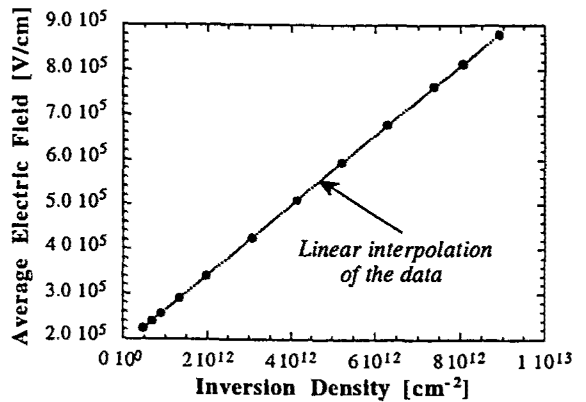

Fig.6 Average electric field vs inversion charge density